# Ultrafast Excited-State Dynamics in the Green Fluorescent Protein Variant S65T/H148D. 3. Short- and Long-Time Dynamics of the Excited-State Proton Transfer[†]

Pavel Leiderman,[‡] Liat Genosar,[‡] Dan Huppert,*[,‡] Xiaokun Shu,[§] S. James Remington,[§] Kyril M. Solntsev,[||] and Laren M. Tolbert[||]

*Raymond and Beverly Sackler Faculty of Exact Sciences, School of Chemistry, Tel Aviv University, Tel Aviv 69978, Israel, Department of Physics and Institute of Molecular Biology, University of Oregon, Eugene, Oregon 97403-1229, and School of Chemistry and Biochemistry, Georgia Institute of Technology, Atlanta, Georgia 30332-0400*

*Received May 11, 2007; Revised Manuscript Received August 16, 2007*

ABSTRACT: Steady-state emission, femtosecond pump−probe spectroscopy, and time-correlated single-photon counting (TCSPC) measurements were used to study the photophysics and the excited-state proton transfer (ESPT) reactions in the green fluorescent protein (GFP) variant S65T/H148D at three pH values: 6.0, 7.9, and 9.5. Selective mutation of GFP caused a dramatic change in the steady-state and excited-state behavior as compared to the wild-type GFP (wt-GFP) studied earlier. An excitation wavelength dependence of the quantum yield of the strong emission band at 510 nm (I* band) indicates the competition between adiabatic and non-adiabatic excited-state proton-transfer reactions. Pump−probe measurements show that the signal buildup probed at 510 nm is biphasic, where 0.8 of the signal amplitude is ultrashort, <150 fs, and 0.2 of the signal decreases with a ∼10 ps time constant. This effect is a summary result of adiabatic ESPT to the carboxylate group of Asp148 and nonradiative processes. When compared with the luminescence of wt-GFP, the steady-state intensity at 450 nm is lower by a factor of about 10. This very weak emission at 450 nm has a nonexponential decay. It is relatively pH insensitive and, at about 25 ps, is almost twice as long as in wt-GFP. The former exhibits a surprisingly small kinetic deuterium isotope effect (KDIE), compared with the KDIE of about 5 for wt-GFP. Such weak proton dependence may indicate that this emission comes from the species not directly involved in the ESPT. In contrast, pH and H/D isotope dependence of the intense nonexponential luminescence decay of the S65T/H148D deprotonated form measured at 510 nm may result from an isomerization-induced deactivation that is accompanied by the proton recombination quenching. The data are complementary to the femtosecond time-resolved emission data obtained by ultrafast fluorescence up-conversion spectroscopy, found in the preceding paper (Shi et al.). The spectroscopic results are discussed on the basis of the detailed X-ray structure of the mutant published in the preceding paper (Shu et al.).

The green fluorescent protein (GFP)[1] of the jellyfish *Aequorea victoria* has attracted great interest as a biological fluorescence marker and one of the few examples of excited-state proton transfer (ESPT) in nature. The wild-type chromophore is characterized by a *p*-hydroxybenzylidene-imidazolone subunit formed from cyclization/autoxidation within a tripeptide unit of the polypeptide sequence consisting of 238 amino acids (*1*). By X-ray diffraction, the chromophore is shown to be protectively housed along a coaxial helix threaded through the center of an 11-stranded $\beta$-barrel (*2*), which effectively secludes it from the aqueous solvent surrounding the protein (*3*). Additional non-covalent coupling of the chromophore to the protein backbone and side chains is facilitated via an extended hydrogen-bonded network (*4*).

At room temperature, GFP exhibits two main absorption peaks with maxima at 398 nm (band A) and 478 nm (band B), which are associated with the chromophore absorption and its conjugate base, as indicated by the increasing intensity of band B at higher pH. Similarly, the two emission peaks in the fluorescence spectrum, a very weak band at 460 nm and a very strong band at 510 nm, are associated with the chromophore and its conjugate base.

The excited-state dynamics of GFP have been studied by several groups (*5*−*10*) using fluorescence up-conversion spectroscopy (about 160 fs time resolution) and other ultrafast techniques. Excitation of the higher energy band leads very rapidly to the lower energy species, and the excited-state interconversion rate shows a large kinetic isotope effect.

Scheme 1 shows a model proposed by Boxer and co-workers (*5*) for the dominant photophysical processes of GFP at 77 K. Upon excitation of the neutral chromophore, A* (R*OH in our notation), it rapidly converts to I* ($R^*O^-$), an anionic chromophore, which is in a nonequilibrium protein environment. The 460 nm emission from the A* decay rate

[†] This work was supported by grants from the Binational U.S.−Israel Science Foundation (to D.H., S.J.R. and L.M.T), the U.S. National Science Foundation (CHE-0456892 to K.M.S. and L.M.T), and the James-Franck German−Israel Program in Laser-Matter (to D.H.).

* Author to whom correspondence should be addressed (telephone 972-3-6407012; fax 972-3-6407491; e-mail: Huppert@tulip.tau.ac.il).

[‡] Tel Aviv University.

[§] University of Oregon.

[||] Georgia Institute of Technology.

[1] Abbreviations: GFP, green fluorescent protein; ESPT, excited-state proton transfer; TCSPC, time-correlated single-photon counting; IRF, instrument response function; KIE, kinetic isotope effect.

10.1021/bi7009053 CCC: $37.00 
Published on Web 10/06/2007

Scheme 1

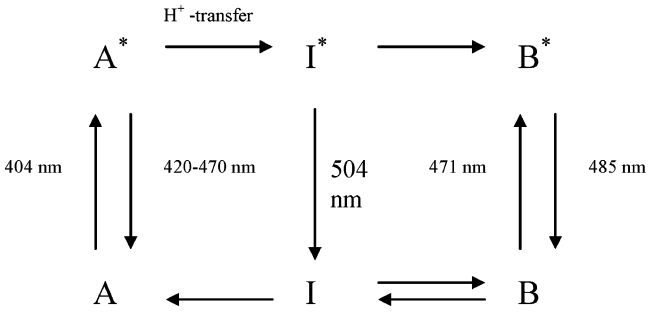


matches the rise in emission from I* measured at about 510 nm. The hydrogen bond network near the chromophore observed in the crystal structure of the GFP is suggested to be responsible for the ESPT (*4*). When B, the ground-state deprotonated chromophore ($RO^-$), is excited at 77 K, it emits at a slightly shifted wavelength from that of I*.

Previous time-resolved studies of GFP focused on the complex decay of the emission at short times up to 150 ps (*5*−*10*), which revealed elementary proton-transfer steps from the excited chromophore to the immediate surrounding bases. Recently (*11*) we have focused our attention on the long-time regime (up to 10 ns). In this regime the time-resolved emission is sensitive to the recombination reaction of the conjugate base and the diffusing proton. We have found that the fluorescence decay of the GFP R*OH band is nonexponential up to 10 ns with a power-law asymptotic limit of $t^{-3/2}$. This effect was observed by us earlier in the ESPT dynamics of various photoacids in solutions (*12*) and was ascribed to the diffusion-assisted reversible geminate recombination that leads to a power-law decay of the fluorescence of the protonated chromophore

$$I_f(t)\, e^{t/\tau_f} \propto [K^*_{eq}/(4\pi D)^{3/2}]t^{-3/2} \quad (1)$$

where $K^*_{eq}$ is the excited-state proton-transfer equilibrium constant, $\tau_f$ is the fluorescence lifetime of the deprotonated form, and $D$ is the mutual diffusion coefficient of a proton and an excited anion. It was a surprise to observe such pronounced diffusion effects in such a conformationally and solvent-restricted photoacid as GFP.

We associate this type of long-time decay with diffusion down the proton-accepting cascade, including the water-22 and Ser205 until Glu222 is reached, which is presumably the end-point of the proton. Because the proton hops from one proton acceptor site to others, under certain circumstances its motion can be approximated by a random walk, and hence a diffusion constant can be assigned to such a motion. The proton can also recombine to its original site, the hydroxyl group of the GFP chromophore, and thus repopulate the protonated form, R*OH. Such a process causes a nonexponential fluorescent decay of this form and asymptotic power-law decay. Using this approach, we have been able to reproduce the fluorescence behavior over the whole time course of the excited state without recourse to the common technique of multiexponential curve fitting (*11*), which has no physical meaning in the case of GFP. However, unlike in homogeneous solution, such diffusion occurs within the "box" created by the protein, in analogy to the H-bond network. We note, however, that the diffusion still follows a three-dimensional power-law dependence, so that additional solvation and proton-transfer modes must be involved. Using our time-resolved data, Agmon has proposed a complex process in GFP in which diffusion of the proton on the surface of the protein with the following exchange with the bulk is invoked (*13*). The temperature-dependent dimensionality of the ESPT (*14*) supports Agmon's model of the proton transfer within GFP: at high temperature a proton might escape to the external solution after a delayed conformational change or become distributed over so many proton wires that its behavior appears to be three-dimensional. At lower temperature the proton migrates along one-dimensional wires on a nanosecond time scale. Interestingly, analysis of the wild-type GFP (wt-GFP) X-ray structure predicts the extension of such a proton wire beyond E222, the acknowledged proton acceptor. The proton wire continues from E222 via the buried D82 to E5, which is located at the bottom of the barrel (*14*).

With these observations in mind, we were intrigued with "moving" the proton acceptor closer to the photoacid by replacing His148 with Asp. For these purposes, we chose the H148D/S65T variant (*15*) and studied its photophysics and photochemistry at three pH levels: 6.0, 7.9, and 9.5. In this variant, the anion of aspartic acid might serve as an effective proton acceptor for the excited state of the chromophore. Indeed, as the accompanying paper attests, such replacement effectively short-circuited the proton-transfer process, leading to an ultrafast proton transfer. Nevertheless, we were able to treat the long-term decay of this process and observe a new process, that is, the strong quenching of the intense green fluorescence band at about 520 nm, which is attributed to the $R^*O^-$ form of the chromophore. Such decay pathways can be analyzed using a combination of twisting-mediated deactivation and proton geminate recombination (*16*, *17*) models.

## EXPERIMENTAL PROCEDURES

Time-resolved fluorescence was acquired using the time-correlated single-photon counting (TCSPC) technique, the method of choice when sensitivity, large dynamic range, and low-intensity illumination are important criteria in fluorescence decay measurements. The TCSPC detection system is based on a Hamamatsu 3809U, photomultiplier, and Edinburgh instruments TCC 900 computer module for TCSPC. The overall instrumental response was about 40 ps (fwhm). Measurements were taken at 10 nm spectral width. The large dynamic range of the TCSPC system (>4 orders of magnitude) enabled us to accurately determine the nonexponential photoluminescence decay profiles of the wt-GFP fluorescence. For excitation we used a cavity-dumped mode-locked Ti:sapphire femtosecond laser (Mira Coherent), which provides short, 80 fs, pulses of variable repetition rate. We used the SHG frequency, over the spectral range of 380−440 nm. Most of the low-pH samples, pH ≤7.9, were excited at about 395 nm. The excitation pulse energy was reduced by neutral density filters to about 1 pJ. We checked the sample absorption prior to and after time-resolved measurements. We could not find noticeable changes in the absorption spectra due to sample irradiation. The time-resolved emission decay curves of the wt-GFP samples were the same after repeated experiments. We thus conclude that, under our irradiation condition, no sample deterioration could be detected.

Scheme 2

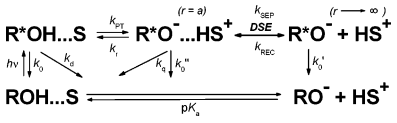


For the pump−probe (transient absorption) experiments reported, we used an amplified femtosecond Ti:sapphire laser system. In brief, laser pulses (50 fs duration, centered near 800 nm with a pulse energy of ~600 $\mu$J) at a 1 kHz repetition rate were generated by a Ti:sapphire-based oscillator (Coherent Mira seed) and amplified by a multipass Ti:sapphire amplifier (Odin Quantronix). Samples were excited by the second harmonic of the amplified laser (~400 nm). To obtain probe pulses we generate a supercontinuum by focusing 1 $\mu$J of the 800 nm pulse onto a 2 nm thick sapphire window. The probe beam signal was measured by a combination of a chopper/lock-in amplifier and computer averaging. Interference filters of 8 nm fwhm bandwidth at the proper wavelength were used in front of the probe beam detector, a silicon photodiode.

Steady-state fluorescence was measured using a FluoroMax-3 spectrofluorometer (Jobin Yvon). Spectra were corrected according to the manufacturer's specifications.

$D_2O$ (99.8% isotopically pure) was purchased from Aldrich. Deionized water (resistivity > 10 MΩ/cm) was used. Synthesis of S65T/H148D was described earlier (*15*). Protein samples of 10 mg/mL, including 0.3 M NaCl, were stored under refrigeration. Samples were prepared by dilution of the stock solution, with either deionized water or $D_2O$, by a factor of about 20. The absorbance at 397 nm was typically 0.1 OD.

The temperature of the irradiated sample was controlled by placing the sample in a liquid $N_2$ cryostat with thermal stability of approximately ±1 K.

## REVERSIBLE AND IRREVERSIBLE DIFFUSION-INFLUENCED TWO-STEP MODEL

Previous studies of reversible and irreversible ESPT processes in solution led to the development of a diffusion-influenced two-step model (*18*−*20*) (Scheme 2). Quantitative agreement was obtained between the model and the experiment.

In the continuous diffusion approach, the photoacid dissociation reaction with the proton transfer to the solvent molecule or other proton acceptor S is described by the formation of the contact ion pair $R^*O^-\cdots HS^+$, with the diffusional separation of the former described by the spherically symmetric diffusion equation (DSE) (*21*) in three dimensions (*18*, *20*). This approach describes diffusional behavior more adequately (*20*) than classical reversible diffusion with the steady-state rate constants of contact ion pair separation ($k_{SEP}$) and recombination ($k_{REC}$). Here, $k_{PT}$ and $k_r$ are the "intrinsic" reversible (adiabatic) dissociation and recombination rate constants at the contact sphere radius, $a$, where $k_d$ is the rate constant of radiationless deactivation competing with the adiabatic dissociation. The overall reaction involves electronically excited species, so one should consider the fluorescence lifetimes: $1/k_0 = \tau_0$ for the acid, $1/k_0' = \tau_0'$ for the base, and $1/k_0'' = \tau_0''$ for the contact ion pair. Usually, $\tau_0''$ is much longer than that for all other chemical and diffusion processes and can be ignored. Generally, this scheme should include one more step associated with the formation of the hydrogen-bonded complex $R^*OH\cdots S$, which was predicted a long time ago (*22*) and found only recently in femtosecond time-resolved experiments on the ESPT from pyranine in aqueous solutions (*23*, *24*). From the X-ray analysis of S65T/H148D it is established that a short hydrogen bond is already preformed in the ground state between the chromophore and Asp148 carboxylate, so this diffusional step can be omitted. The back protonation may also proceed by a nonadiabatic irreversible pathway involving proton quenching with a rate constant $k_q$ (*25*−*29*). From an analysis of the time-resolved data of the S65T/H148D $R^*O^-$ form we have found that quenching of the $R^*O^-$ band is strong and hence strongly affects the time-resolved emission profile of $R^*O^-$. The relative quantum yield of the $R^*O^-$ emission when excited initially by a photon to the R*OH form is smaller by a factor of 3 than the excitation of the $RO^-$ form at 470 nm. The smaller quantum efficiency is indirect evidence of the quenching of $R^*O^-$ by the geminate proton.

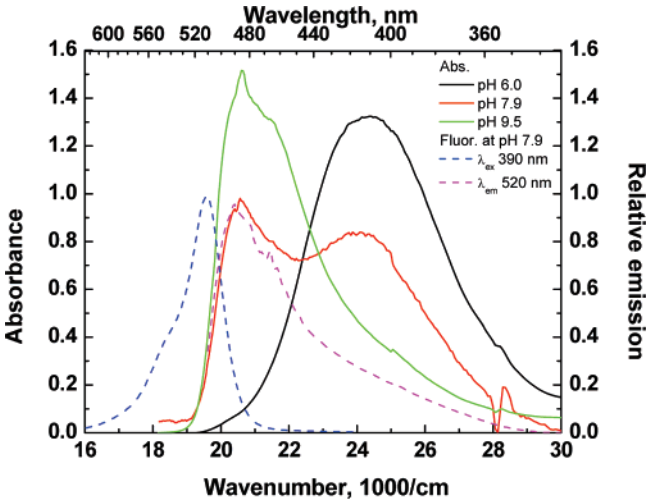


FIGURE 1: Absorption spectra of the GFP variant S65T/H148D in $H_2O$, at three pH values: 6, 7.9, and 9.5. Also shown are corrected excitation and emission spectra at pH 7.9.

## RESULTS

*Steady-State Measurements.* Figure 1 shows the absorption spectra of GFP variant S65T/H148D samples in $H_2O$ at three pH values: 6, 7.9, and 9.5. (The spike at about 490 nm is an instrumental artifact.) The two defined absorption bands of ROH and $RO^-$ are located at 24200 and 20500 $cm^{-1}$ (413 and 488 nm), respectively, demonstrating a significant bathochromic shift from the wt-GFP absorption bands. The pH dependence of the spectrum clearly indicates that a ground-state acid−base equilibrium $ROH \leftrightarrow RO^- + H^+$ exists, with $pK_a \sim 8$. This effect observed earlier (*15*) places the mutant among useful ratiometric dual absorption pH sensors. Wt-GFP does not show pH dependence of its absorption in this pH region.

The same figure shows the corrected excitation spectra and the emission of GFP variant S65T/H148D at pH 7.9. The full profile of an excitation spectrum of the $R^*O^-$ emission band (measured at 520 nm) does not follow the absorption spectrum. When excited at about 400 nm, the

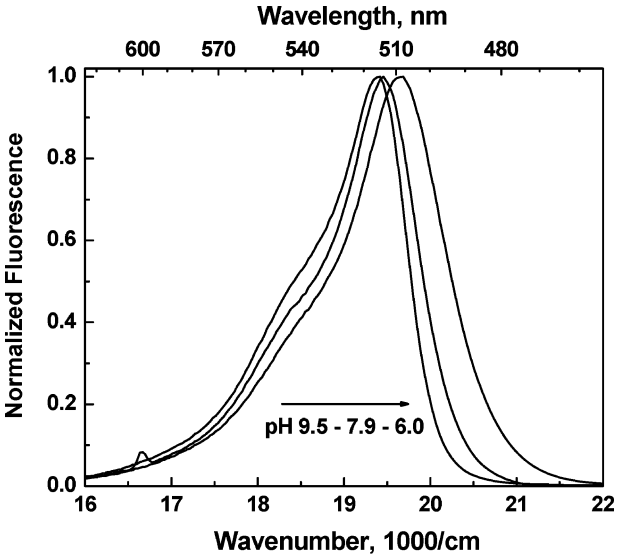


FIGURE 2: Steady-state emission spectra of the GFP variant S65T/H148D in $H_2O$, at three pH values: 6, 7.9, and 9.5.

excitation quantum efficiency is about one-third of that of direct excitation at 480 nm, the band maximum of the $R^*O^-$ $S_0-S_1$ transition. In the case of a fast proton-transfer rate, $R^*OH \rightarrow R^*O^- + H^+$, this low value indicates that the excited-state protolytic cycle also includes loss of excitation energy at some proton-transfer step, which causes fluorescence quenching of the $R^*O^-$ emission (see Scheme 2). The excitation of the emission spectra was at 390 nm. The emission spectrum position and width depend on the pH values (Figure 2). The lower the pH, the larger the blue shift of the band position. At pH ~6, the band position shifts by about 270 $cm^{-1}$ to the blue. The width increases from about 950 $cm^{-1}$ at pH 7.9 to about 1100 $cm^{-1}$ at pH 6. The latter emission can be related to the I* band, whereas the former relates to the directly excited anion (B* band).

Figure 3a shows the steady-state emission spectra of the $R^*O^-$ band of variant S65T/H148D at pH 7.9 when excited at two excitation wavelengths, 390 nm, the $S_0-S_1$ transition of the ROH band, and 470 nm, the direct excitation of the $RO^-$ form. As seen in the figure, there is a large difference in the spectral width when excited at the ROH or the $RO^-$ absorption bands. After excitation to the ROH band, the $R^*O^-$ emission is formed by the excited-state protolytic reaction (I* band), and the emission spectrum is wider and less structured than that after direct excitation at 470 nm (B band), the peak of the $RO^-$ form absorption band. The same effect is observed at pH 6. For common fast photoacids in bulk solvents at room temperature the width of the $R^*O^-$ emission band is identical upon direct and indirect excitation. Unlike its S65T/H148D mutant, the wt-GFP shows an opposite dependence of the $R^*O^-$ bandwidth on the excitation wavelength (Figure 3b). The $R^*O^-$ emission, when excited at 470 nm, is broader than when excited at the ROH absorption band at 390 nm. To make the difference between wt-GFP and S65T/H148D more illustrative, we present two additional graphs. Figure 3c demonstrates the expanded blue edge of the overlapped and normalized fluorescence spectra of wt-GFP and S65T/H148D. The relative emission of the high-energy band is larger for wt-GFP, whereas for S65T/H148D it is almost negligible. Figure 3d shows the overlapped spectra from Figure 3a,b. All *X*-scale values were shifted to match all maxima. It is clearly seen that the width of the emission spectra of the excited anion formed due to ESPT is much for larger for S65T/H148D, whereas the spectra of the directly excited anions are almost identical for wt-GFP and S65T/H148D.

*Time-Resolved Measurements. (a) Pump−Probe.* The steady-state spectrum of S65T/H148D at pH 6.0 (Figure 3c) shows very weak emission in the 440−460 nm region where the R*OH signal is expected. The quantum yield of this emission was much lower than that of wt-GFP. Therefore, a very fast decay of the protonated form of the chromophore is expected, with the ESPT as one of the important deactivation channels. Simultaneously, a very fast buildup of conjugated anion signal is also anticipated.

Figure 4 shows the pump−probe signal (transient absorption, $\Delta A$) of a pH 6.0 aqueous solution of S65T/H148D. The solution was pumped at 400 nm with a ~100 fs pulse at 1 kHz and probed at 510 nm generated by supercontinuum, the wavelength close to $R^*O^-$ emission maximum. As seen in Figure 4, the signal is negative and 80% of its amplitude is gained within the time resolution of the experimental setup of about 150 fs (the cross-correlation fwhm is 150 fs). The fast component is followed by a slower phase. The minimum point is at about 40 ps. Approximately 20% of the signal is composed of a nonexponential growth with an average time of 10 ps. At longer times ($t > 50$ ps) the signal intensity decreases with a time constant of a few hundred picoseconds that fits the decay time observed in the time-resolved emission measured at 510 nm by the TCSPC technique and is shown in Figures 4 and 6. The pump−probe signal growth period of S65T/H148D measured at 510 nm is much shorter than what was found in wt-GFP under similar conditions (*11*). This ultrafast generation time is in very good agreement with the ultrafast decay and rise also observed in the fluorescence up-conversion signal of Boxer and Remington (*30*).

*(b) Time-Correlated Single-Photon Counting.* Despite the very weak steady-state R*OH emission at 450 nm, a long-time accumulation of TCSPC signals results in decay curves with a good signal-to-noise ratio. Figure 5 shows the time-resolved emission of the R*OH form, measured at 450 nm for the GFP variant S65T/H148D, at the pH values of 6.0, 7.9, and 9.5. All exhibit a nonexponential nature of the decay curves at longer times. The overall decay profile of the three samples varies only slightly at different pH values. Also, almost no isotope effect is observed at all pH values (data not shown). In Figure 5, we also plot the instrument response function, which has a 40 ps fwhm (*31*). It is important to note that all excited-state processes that are significantly faster than the latter time value could not be detected, and the ultrafast emission component that is complementary to <150 fs pump−probe component may go undetected.

Figure 6 shows the time-resolved emission of the $R^*O^-$ form of the variant S65T/H148D, measured at 520 nm (the $R^*O^-$ emission band maximum is at 510 nm) at different pD values and excited at ~400 nm, the ROH form absorption maximum. In protic solvents the kinetic behavior of $R^*O^-$ was essentially the same. For comparison, we add a similar emission decay curve of wt-GFP in $D_2O$ excited at 400 nm and measured at 512 nm. In contrast to the wt-GFP signal, which has a detectable rise time and almost single-

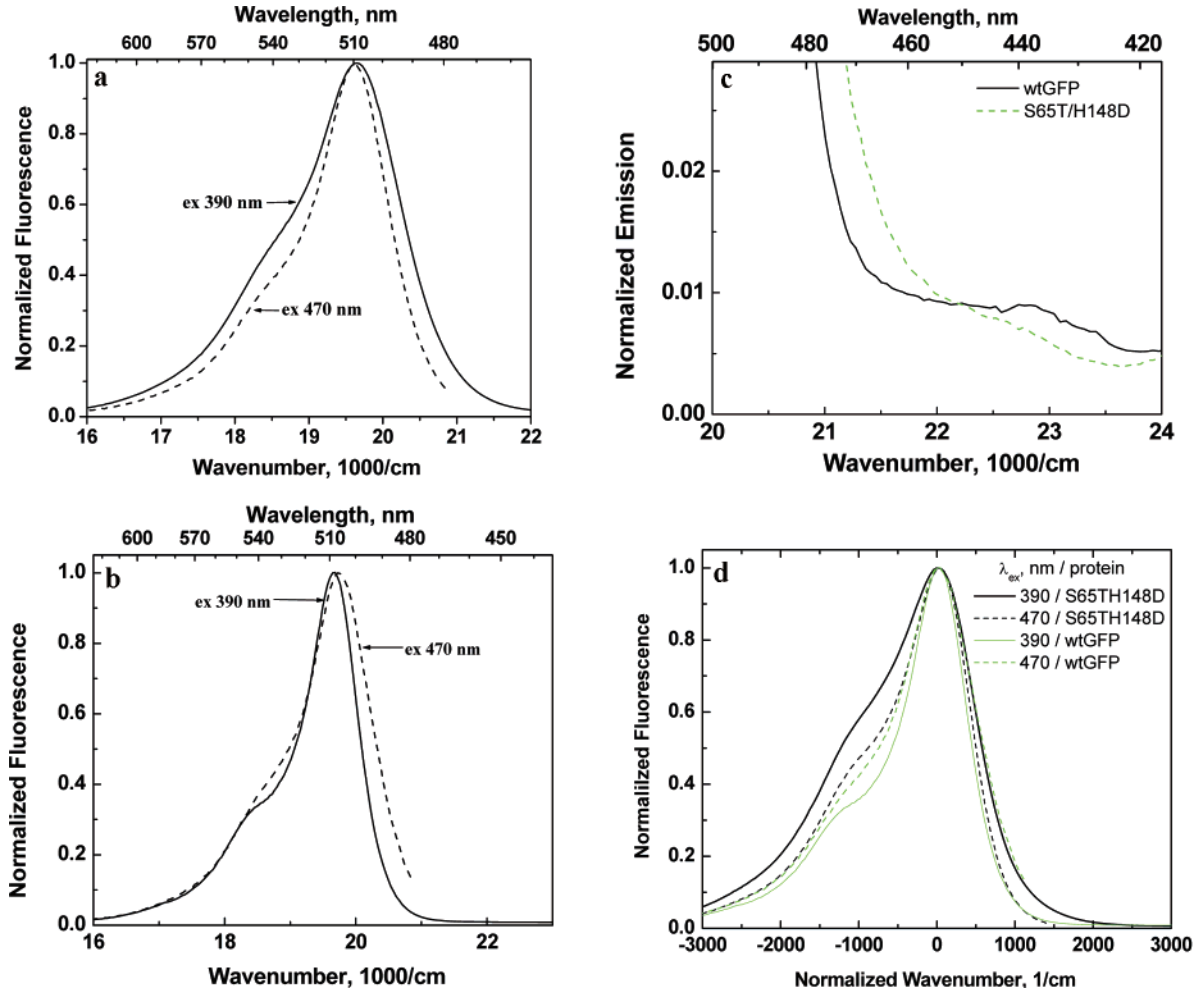


FIGURE 3: Steady-state emission spectra at two different excitation wavelengths, 390 and 470 nm: (a) variant S65T/H148D, pH 6; (b) wt-GFP; (c) high-energy part of the overlapped S65T/H148D and wt-GFP spectra; (d) overlapped emission from (a) and (b). All spectra are normalized to the *X*-scale values corresponding to the emission maxima.

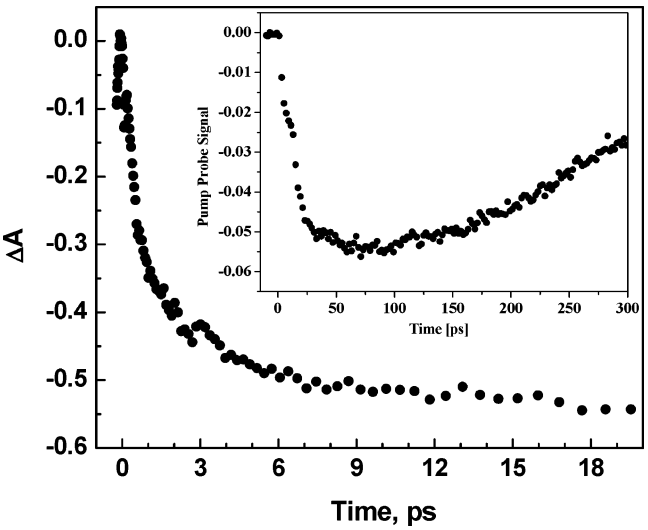


FIGURE 4: Pump−probe signal of S65T/H148D in water at pH 6.0 monitored at 510 nm.

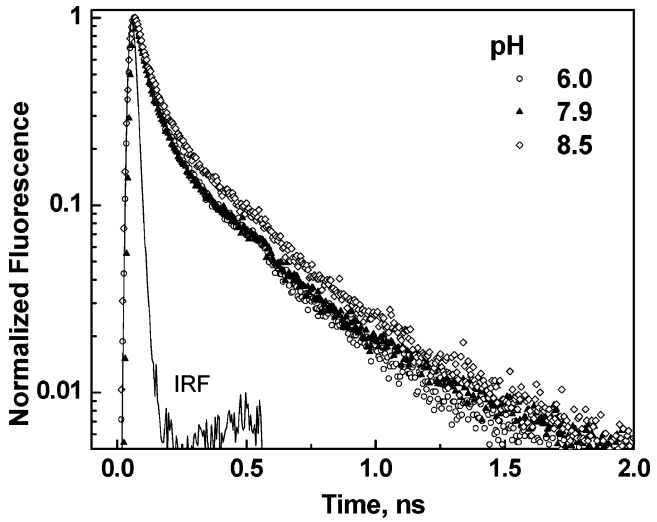


FIGURE 5: Time-resolved emission of the S65T/H148D R*OH form measured at 450 nm at three pH values: 6, 7.9, and 9.5.

exponential decay, the GFP variant R*O$^-$ emissions are quenched, have concave shapes on a semilog plot, and have no detectable rise time. Our pump−probe data discussed above demonstrate an ultrafast nature of this rise time. It can also be seen that the lower the pD (or pH), the larger the decay rates of the R*O$^-$ form fluorescence of the variant. Deuterium exchange slows the decay of indirectly excited R*O$^-$ as shown in Figure 7.

*(c) Temperature Dependence of the Steady-State and Time-Resolved Emission.* To reveal the origin of unusually fast deactivation of the GFP chromophore caused by mutation, we performed steady-state and picosecond time-resolved

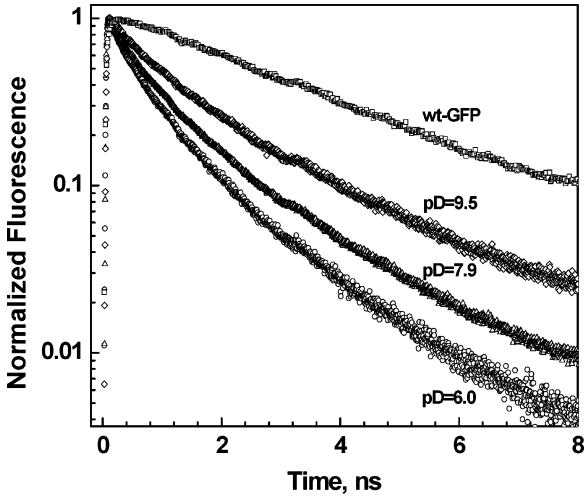


FIGURE 6: Time-resolved emission of the S65T/H148D R*O$^-$ form measured at 520 nm at three pD values: 6, 7.9, and 9.5. The analogous signal of wt-GFP measured in $D_2O$ at 512 nm is given for comparison.

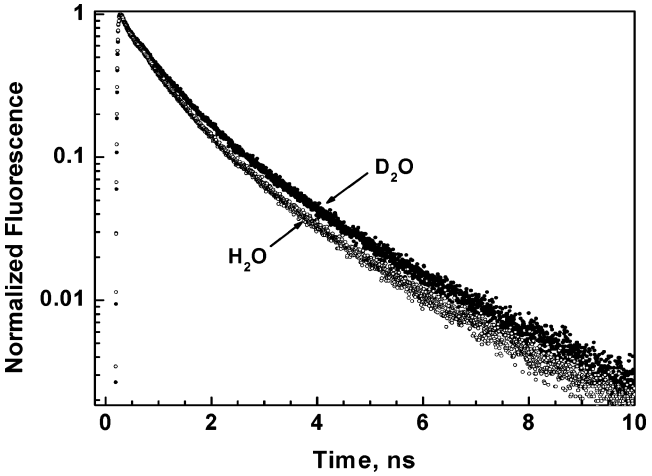


FIGURE 7: Time-resolved emission of the S65T/H148D R*O$^-$ form measured at 520 nm in $H_2O$ and $D_2O$ at pH 6 and pD 6.

measurements in a wide range of temperatures. Figure 8 shows the temperature dependence of the steady-state emission of a pH 6 S65T/H148D sample. The latter was excited at 400 nm by a low-power high-repetition rate (500 kHz) with 100 fs pulses. As the temperature decreases, the band peak at 510 nm shifts to the blue. Below 240 K a new emission band appears in the spectrum with a peak position at about 485 nm. The overlap of the bands as seen in the spectra is large, and thus it is hard to distinguish the two separate bands. The lower the temperature, the stronger is the new emission band. In the accompanying paper (*30*) analogous measurements in 60% glycerol/water mixtures resulted in much greater intensity of the high-energy emission peak at low temperatures. A detailed analysis of the steady-state spectra at various temperatures is given under Discussion.

Panels a and b of Figure 9 show the time-resolved emission of S65T/H148D at various temperatures measured at 445 and 510 nm, respectively. The 510 nm time-resolved emission at room temperature shown in Figure 9b exhibits an ultrafast rise time of the R*O$^-$ band (within the instrument response function) followed by a nonexponential decay. The long component of this emission band decay is 2.64 ns,

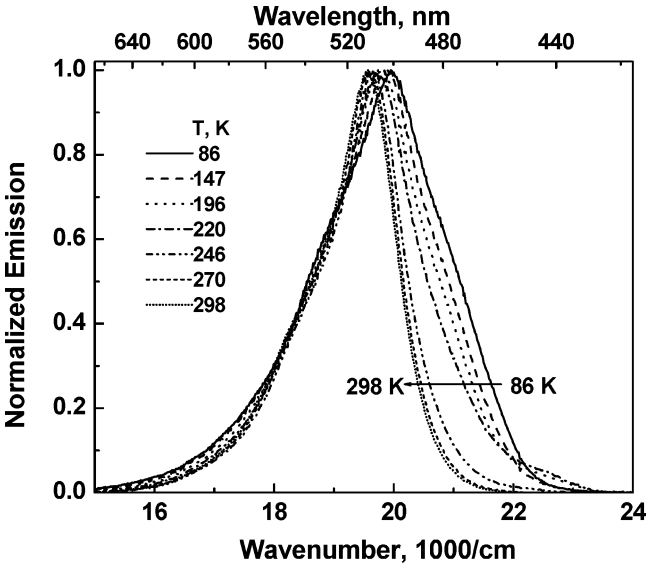


FIGURE 8: Steady-state emission spectra of the GFP variant S65T/H148D in $H_2O$ at pH 6.0 and various temperatures.

slightly faster than the lifetime of the I band of the wt-GFP. As the temperature decreases, the nonexponential fast decay components becomes slower. At about 160 K, the decay is almost exponential with a 2.7 ns decay time. At the lowest studied temperature, 86 K, the 510 nm emission curve exhibits a biphasic growth of fast and slow components. The rise time of the slow component with an amplitude of about 0.5 is about 300 ps. The slow component may arise from the large scattering of the frosted sample of both the excitation pulse and the fluorescence. The sample has a thickness of about 4 mm and is acting as a frosted glass.

Figure 9a shows the TCSPC signal measured at 445 nm. The signal intensity is much lower than the signal at 510 nm at all temperatures. At temperatures below 240 K, the signal intensity is strong, with photon counting rates of about 0.3 of that measured at 510 nm. The average decay times are longer as the temperature decreases. At temperatures below 130 K the signal decays exponentially with a lifetime of 2.7 ns. Figure 9b demonstrates the R*O$^-$ lifetime increase with temperature decrease. At 86 K the decay is almost monoexponential with the lifetime of 2.7 ns, very close to that of 445 nm decay.

## DISCUSSION

The main findings of this spectroscopic study on the GFP variant S65T/H148D can be summarized as follows:

1. The pump−probe signal pumped at 400 nm (the protonated absorption band) and probed at 510 nm (deprotonated form emission band) is biphasic with a dominating (80%) short-time component, $\tau < 150$ fs, followed by a minor longer component of about 10 ps.

2. Surprisingly, the kinetic isotope effect (KIE) of the fluorescence decay in the R*OH band is very small compared with the KIE of about 5 for wt-GFP. The large isotope effect in the latter case is a distinctive indication of a kinetically limiting proton-transfer process in the excited state.

3. The emission spectrum of wt-GFP, excited at 400 nm, shows a very weak, but detectable, emission band at 450 nm (relative intensity with respect to the R*O$^-$ is 0.002). This weak band is attributed to the R*OH band emission.

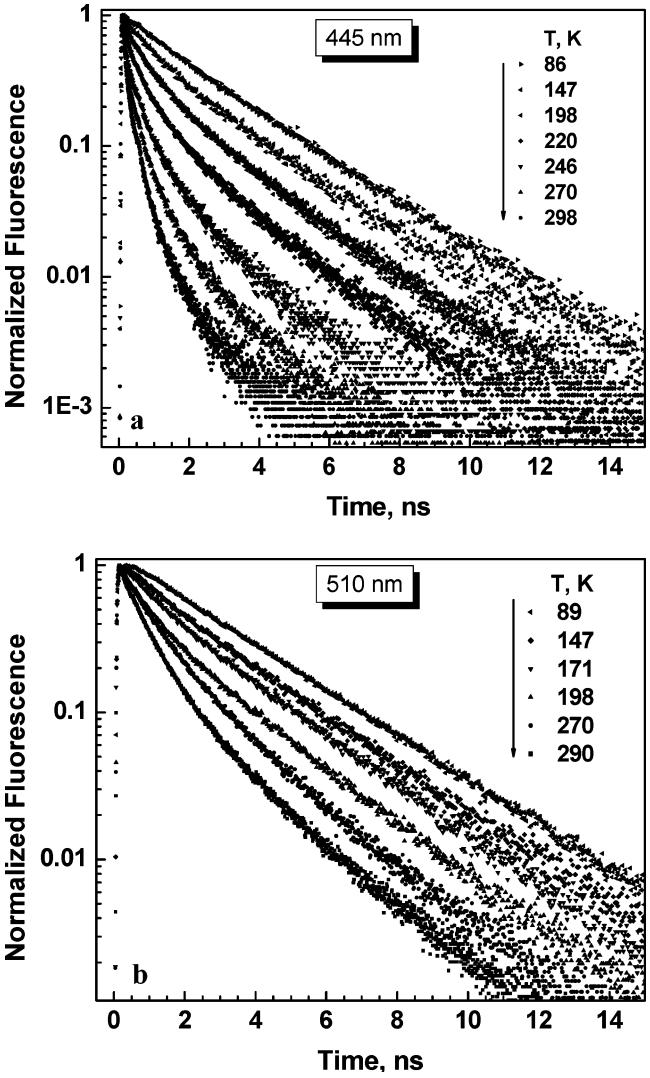


FIGURE 9: Time-resolved emission of the S65T/H148D R*OH form at pH 6.0 and various temperatures: (a) measured at 445 nm; (b) measured at 510 nm.

Its low intensity is attributed to the ~10 ps proton transfer, compared to the ~3.0 ns excited-state lifetime of $R^*O^-$ at 510 nm and the lifetime of R*OD in deuterated samples (at low temperature). The intensity of such a blue band in S65T/H148D is almost negligible. From the above-mentioned findings of the ultrafast pump−probe signal at 510 nm, the lack of KIE, and the lack of a blue band in S65T/H148D, we conclude that in S65T/H148D both the proton transfer and radiationless transition rates of the R*OH excited state are ultrafast and thus strongly affect both the kinetics and the steady-state emission.

4. When excited at 400 nm (the ROH band) the fluorescence quantum yield of the $R^*O^-$ band at 510 nm is smaller by a factor of about 3 than after direct excitation at 475 nm. The $R^*O^-$ fluorescence is mildly quenched in S65T/H148D, and the time-resolved luminescence decays nonexponentially. Both isomerization and proton (deuteron) quenching influence the time-dependent quenching rate. In wt-GFP these processes are negligible and $R^*O^-$ fluorescence decays almost exponentially.

We will discuss the steady-state and time-resolved spectroscopic data on the basis of detailed X-ray structure of S65T/H148D provided in the preceding paper (*32*).

*Steady-State Room Temperature Measurements.* We note that the absorption maxima of the ROH (A) band in S65T/H148D is 18 nm red-shifted as compared to wt-GFP and >40 nm red-shifted compared with that of a model chromophore *p*-HBDI in the wide array of solvents (*33*). A combination of several factors such as hydrogen-bonding and electrostatic interactions within the protein, as well as slight chromophore twisting, could be responsible for bathochromic shifts of the neutral chromophore absorption in the protein. In the case of the present mutant such an enormous shift is most probably caused by partial proton transfer from Tyr66 hydroxyl to the carboxylate of Asp148 as can be judged by the X-ray data on the short hydrogen-bonded complex between these acid−base groups. We demonstrate below that the existence of the strong hydrogen-bonded complex already in the ground state results in ultrafast (<200 fs) ESPT, an effect unusual for proteins, but well studied for small organic molecules (*34*−*40*).

The remarkable pH sensitivity of the GFP S65T/H148D variant was discovered earlier (*15*). In contrast to wt-GFP, the position and width of the steady-state emission spectrum are very sensitive to pH and excitation wavelength. For both pH 7.9 and 6.0, there is a large difference in the spectral width, when excited at the ROH or the $RO^-$ absorption bands. The width of the emission spectrum is larger when excited to the ROH, and the $R^*O^-$ emission band is formed by the excited-state protolytic reaction. At 470 nm excitation, the maximum of the $RO^-$ absorption band, the emission spectrum is relatively narrow and more structured. Figure 3d shows that, in wt-GFP, the wavelength dependence is the opposite of that of the variant S65T/H148D. The $R^*O^-$ emission, when excited at 470 nm, is broader than its emission when excited at the ROH absorption band at 390 nm.

Why is the emission spectrum of ESPT product broader in S65T/H148D? We observed a similar effect (*41*) in comparing the emission from *p*-HBDI and wt-GFP anions. Using the model combining inhomogeneous broadening and a coordinate-dependent sink term (*42*), it was established that in free chromophore the emission spectrum is much wider and radiationless transition is much stronger than in protein-embedded chromophore. These phenomena are consistent with the twisting about the double bond of the chromophore (*43*). By X-ray analysis it is known that at neutral pH the chromophore is much more twisted in the S65T/H148D mutant than in wt-GFP (*32*), probably resulting from somewhat larger conformational freedom. The difference is smaller for the deprotonated chromophore. Another explanation may deal with the chromophore excited-state relaxation. As shown below, the ESPT process in the mutant is ultrafast and probably occurs from an unrelaxed state, which may lead to a wider distribution of the excited-state fluorescent products. Various degrees of conformational freedom show themselves not only in $R^*O^-$ emission spectral width but in the decay kinetics as well (see below).

*Pump−Probe Measurements.* The 510 nm emission band in GFP (the I* band) is attributed to the deprotonated form. A plausible explanation for the <150 fs fast generation of the I* band from the A* band in the case of S65T/H148D is an ultrafast proton-transfer process. The X-ray structure of the low-pH sample shows the distance between the chromophore Tyr66 oxygen and the carboxylic oxygen of Asp148

to be only 2.3 Å (*32*). This short distance suggests the proton of the phenolic hydroxyl group is strongly hydrogen bonded to the aspartic acid already in the ground state. In such a case, excitation of the ROH band might lead to an immediate proton transfer on the upper surface. Similar ultrafast proton-transfer rates are observed not only in some intramolecular excited-state proton-transfer processes (*35*−*40*) but also in bimolecular ESPT from an excited hydroxyaromatic photoacid to acetate anion at high concentrations of acetate (1−4 M), at which ground-state HB complex is preformed (*23*).

It is important to realize that the observed <150 fs rate does not solely reflect the magnitude of the adiabatic ESPT rate constant. We note that the direct absorption-normalized excitation of the $RO^-$ band leads to a much stronger emission of the I band than excitation of the A band (ROH band), despite the very fast formation of the former. The asymmetry in the excitation behavior is because ESPT-induced deactivation and/or nonradiative processes (geminate proton quenching) shown in Scheme 2 may compete with the adiabatic ESPT processes. Such behavior was observed for several hydroxyaromatic photoacids, and a kinetic analysis of the competitive reaction scheme was performed.

According to Scheme 2 the quantum efficiency of the adiabatic protolytic dissociation of R*OH ($\eta$) is defined as (*44*, *45*)

$$\eta = k_1/(k_1 + k_d) = k_{SEP}/(k_{SEP} + k_{NR}) \quad (2)$$

$$\eta = (\varphi'_N/\varphi'_0)(\tau'_0/\tau'_N)/(1 - \tau_N/\tau_0) \quad (3)$$

where $\varphi'_N$ ($\tau'_N$) and $\varphi'_0$ ($\tau'_0$) are fluorescence quantum yields (lifetimes) of $R^*O^-$ after indirect and direct excitation, $\tau_N$ is the decay time of R*OH and the rise time of $R^*O^-$, $1/\tau_N = 1/\tau_0 + k_d + k_1$, $k_1$ is the apparent ("steady-state") ESPT dissociation rate constant, $k_{NR}$ is the nonradiative rate constant of the contact ion pair, which includes both proton quenching with rate constant $k_q$ and nonradiative component of the decay constant $k_0''$. The apparent ESPT rate constant $k_1$ can be expressed in terms of the rate constants of the elementary reactions presented in Scheme 2:

$$k_1 = k_{PT}\, k_{SEP}/(k_r + k_q + k_{SEP}) = k_{PT}/(1/\eta + k_r/k_{SEP}) \quad (4)$$

We have found experimentally that $\varphi'_N/\varphi'_0 = 0.33$, and the ratio of amplitude-weighted average decay times $\langle\tau'_0\rangle/\langle\tau'_N\rangle = 2.0$, whereas $\tau_N \ll \tau_0$. This leads to the ESPT quantum efficiency $\eta = 0.66$. It shows that the short rise time of the pump−probe signal measured at 510 nm after excitation of the ROH band by a 400 nm pump pulse is only partially controlled by the proton-transfer rate constant. The large nonradiative rate constant, with a rate faster than 1 $ps^{-1}$, was also observed in the synthetic chromophore, *p*-HBDI, in aqueous solutions and other liquids. Michel-Beyerle (*46*), Meech (*9*), and Van Grondelle (*47*), as well as some of us (*42*), observed that the radiationless rate is nonexponential in both the neutral and the deprotonated form of *p*-HBDI. Van Grondelle (*47*) found that the neutral form decays to the ground state more quickly than the deprotonated form. The fast components of the radiationless decay are a few hundred femtoseconds, similar to the fast components found in the pump−probe signal of S65T/H148D shown in Figure 4.

A possibility of the effective ESPT-induced deactivation in GFP chromophores was proposed in ref *48*. It was suggested that the initially prepared $^1\pi\pi^*$ state intersects with the $^1\pi\sigma^*$ electronic state along the proton-transfer coordinate, resulting in proton-coupled electron transfer. We have no experimental evidence supporting this mechanism.

*Quenching of the R*O⁻ Form of the Chromophore.* In the previous section we have demonstrated how selective mutations changed the mechanism of the primary ESPT in GFP. Now we turn to the excited-state behavior of the conjugated excited deprotonated species. The photophysics and photochemistry of the deprotonated fluorophores of the mutant also differ strongly from those of the parent wt-GFP. In contrast to the latter, the $R^*O^-$ fluorescence decay of S65T/H148D is nonexponential. First, it is important to note that the $R^*O^-$ decay is nonexponential even at basic pH, at which the GFP chromophore anion is excited directly. Therefore, the high pH value rules out possible excited-state proton quenching in this sample. A fit to the multiexponential law resulted in two major components with lifetimes of 0.68 and 2.64 ns, with a ratio of amplitudes of 1.5. Biexponential fluorescent decays of directly excited $R^*O^-$ forms of various GFP mutants were reported recently (*49*). The authors suggested that the major mechanism of quenching that leads to shortening of GFP $R^*O^-$ lifetimes is the rotation of phenyl versus imidazolone rings, or a concerted "hula-twist" motion. This is a proposed mechanism of the excited-state deactivation of GFP chromophore in solution (*9*, *42*, *43*). The same authors explained biexponential $R^*O^-$ decay in various GFP mutants by heterogeneity of the chromophore microenvironment. This may not necessarily be the case, because one of us demonstrated in the previous paper (*42*) that at low temperatures the $R^*O^-$ fluorescence decay of a GFP model chromophore may be close to biexponential even in homogeneous solution.

At lower pH the $R^*O^-$ decay becomes even faster (Figure 6); that is, the fluorescence of this form is quenched even more, decreasing the lifetimes of two major decaying components to 0.40 and 1.55 ns. The same effect was observed by Jung et al. for directly and indirectly excited GFP mutants at the same pH (*49*). There are several options for the additional fluorescence quenching of $R^*O^-$ upon indirect excitation:

First, it is known that the lifetime of the GFP anion chromophore depends on mutation, which may vary the microenvironment in the vicinity of the chromophore, for instance, steric hindrance or polarity. From X-ray studies of wt-GFP and its several mutants at different pH (*32*), we know that the degree of chromophore twisting significantly increases in the order wt-GFP − S65T/H148D pH 10 − S65T1/H148D pH 6.5. Recent quantitative theory of isomerization-induced quenching in GFP chromophores (*42*) may explain the decrease of $R^*O^-$ fluorescence lifetime in this order if one assumes that pretwisted chromophores reach the conical intersection point more easily. Therefore, the structural properties of the chromophores in proteins at different pH values very well correlate with their photophysical characteristics.

Second, pH and H/D isotope effects on the S65T/H148D $R^*O^-$ emission decay measured at 520 nm and excited at 400 nm were found (Figures 6 and 7). In the previous paragraph we demonstrated that the pH dependence of the

$R^*O^-$ fluorescence lifetime can be a result of structural perturbation of the chromophore in the protein. However, small but detectable H/D isotope effects suggest that proton quenching can be also involved in the deactivation paths. Similar effects observed for several hydroxyaromatic photoacids were associated with nonadiabatic geminate proton quenching. The branching between the adiabatic and nonadiabatic protonation has been attributed to competing processes, protonation on the parent oxygen atom and on the aromatic ring, such as in 1-naphthol (*27*, *45*, *50*), or on various substituents and functional groups. The results we observe may suggest that proton quenching results in a zwitterion (*51*), which is predicted to be nonfluorescent. Thus, proton quenching can also account for some portion of the internal conversion for GFP chromophore, both in solutions and in protein matrices. Clearly, there is an analogy between such behavior for GFP and other photoacids. In the case of the wt-GFP no significant proton quenching was observed, probably because the hydrogen-bond network surrounding the chromophore does not favor proton diffusion to the imidazolinone ring of the excited chromophore. Unfortunately, we could not utilize our usual procedure of nonlinear numeric fitting of $R^*O^-$ decay curves to the time dependence of anion emission (Scheme 2) using the SSDP program because of the large number of unknown kinetic and thermodynamic parameters required for such fitting.

As seen in Figure 7, the quenching rate is smaller in the deuterated sample. To evaluate qualitatively the effect of deuteration on the $R^*O^-$ decay profile, we fit these decay curves to a polyexponential expression. The ratio of average lifetimes $\langle\tau'_N\rangle_D/\langle\tau'_N\rangle_H$ was about 1.22. This fact indicates that the quenching of the $R^*O^-$ band is related to the proton/deuteron that is transferred to the protein and perhaps reacting with the imidazolone ring. The slow quenching rate of the $D_2O$ sample might be due to several reasons. The first is a slower diffusion constant of the deuteron and, thus, later arrival time of the deuteron at the target, that is, the attack position on the imidazolone ring. The second is that the rate constant of the attack ($k_q$, the quenching rate constant) is smaller for the deuteron. The quenching rate constant, $k_q$, of deuterated photoacids in a homogeneous solution of $D_2O$ is slower (*52*, *53*).

The possible mechanism of an increased proton quenching in S65T/H148D mutant as compared to the wt-GFP is given below. In the X-ray structure of the S65T/H148D mutant at pH 5.6 (*32*) water molecules w28 and w29 are close to the imidazole ring. The water may form a channel or a bridge in which the proton/deuteron can diffuse from the phenol toward the heterocyclic nitrogen atom, which may act as a quenching target on the imidazole ring. The proton, being transferred initially to Asp148, may "leak" to the proton wire that exists in S65T/H148D, finally reaching the imidazole ring. The contribution of the proton quenching to the deactivation mechanism is probably not large because the H/D isotope effect on the $R^*O^-$ fluorescence lifetime is small. This is understandable, however, taking into account that the primary ESPT does not go directly to this proton wire, such as in wt-GFP, and only a small fraction of transferred protons can reach it. We are intrigued whether the efficient proton fluorescence quenching has the lower dimension of such a channel as compared to a three-dimensional open space such as in homogeneous solution (*14*). In a low dimensional space, which is also limited in its total volume as well as each of its "walls", the random walker (the proton or the deuteron) has a much larger probability of hitting the target. The kinetic analysis of S65T/H148D fluorescence decay curves based on this model is in progress.

The $R^*O^-$ decay at pH 7.9 is intermediate between those at pH 6.0 and 9.5. It can be easily explained by the ground-state $ROH \leftrightarrow RO^- + H^+$ equilibrium. At pH 7.9 the absorbance at 400 nm is a combination of neutral and anionic form of the chromophore (Figure 1). Therefore, the observed $R^*O^-$ decay is a superposition of the directly and indirectly excited anion.

To summarize, both isomerization and proton quenching may be responsible for an enhanced $R^*O^-$ deactivation in the S65T/H148D mutant. A number of additional experiments including time-resolved IR and Raman as well as structural measurements are required to prove these hypotheses at the molecular level.

*Low-Temperature Steady-State Emission Spectrum Analysis.* To clarify the nature of the ultrafast ESPT at room temperature we measured steady-state and time-resolved emission at lower temperatures. Upon cooling, we observed a blue shift of the $R^*O^-$ emission maximum (Figure 8) and the appearance of a high-energy shoulder at about 470 nm, which we associate with the A* (R*OH) emission band. One may assume that the ESPT slows at low temperatures. However, no detectable rise time was observed in the time-resolved emission curves of $R^*O^-$ even at 89 K. This is in a good agreement with our hypothesis of a practically barrierless ESPT in S65T/H148D. A temperature decrease leads also to an increase of $R^*O^-$ decay time, whereas the decay profile becomes almost single exponential (Figure 9b). This effect was observed also for the *p*-HBDI anion (*14*) and was explained by the freezing of the isomerization process in the chromophore.

Now we will discuss the nature of 445−480 nm emission and its decay at various temperatures. As was mentioned before, at room temperature the steady-state emission in this spectral region is extremely weak. The time-integrated decay profiles and the steady-state intensity increased as the temperature decreased, but at no temperatures did the 445 decay match the 510 nm ultrafast risetimes. Taking this into account, we propose that the very weak time-resolved emission detected by TCSPC at 445 nm is related to a species not directly linked to ESPT dynamics. The lack of pH and H/D dependence may reflect the existence of additional deactivation pathways other than ESPT. It is tempting to assume that two conformers differing in their ESPT reactivity exist in the protein. However, X-ray data show no evidence of a second conformer. We note the possible relevance of Vohringer's hypothesis (*8*) suggesting that the intra- and intermolecular transfer of excess vibrational energy transfer may lead to nonreactive degrees of freedom.

An alternative explanation is based on the existence of the proton wire very similar to that of in wt-GFP (*32*). Whereas the ESPT occurs primarily to the carboxylate of the Asp148 residue almost instantly upon excitation, the transferred proton may then "leak" to that wire, giving rise to a reprotonation−deprotonation cycle. This may account for the small portion of the slow kinetics in TCSPC and pump−probe data due to geminate recombination process.

The very low isotope effect on the lifetime of this component can be evidence of the insignificance of these processes in the rate-limiting proton-transfer steps.

## SUMMARY AND CONCLUSIONS

Steady-state emission and time-resolved techniques such as pump−probe spectroscopy as well as time-correlated single-photon counting (TCSPC) were used to study the excited-state proton-transfer reaction in green fluorescent protein variant S65T/H148D at three pH values: 6.0, 7.9, and 9.5. Unusually fast ESPT is explained on the basis of protein crystal structure, which demonstrates a preformed hydrogen bond between the chromophore and the Asp148 carboxylate. The kinetic isotope effect (KIE) of the R*OH decay rates is surprisingly very small as compared to the KIE of about 5 for wt-GFP. Fluorescence of the deprotonated form, $R^*O^-$, is quenched in the S65T/H148D mutant, demonstrating pH and H/D dependence of this process. Both photoisomerization and proton quenching may be responsible for an enhanced $R^*O^-$ deactivation in S65T/H148D mutant. The latter deactivation mechanism may include the diffusion of the transferred proton from the phenol ring to the imidazolone ring of the chromophore forming the nonfluorescent zwitterion.

## ACKNOWLEDGMENT

We thank Professors N. Agmon and M. Gutman for their helpful discussions and fruitful suggestions.

## REFERENCES

1. Cubitt, A. B., Heim, R., Adams, S. R., Boyd, A. E., Gross, L. A., and Tsien, R. Y. (1995) Understanding, improving and using green fluorescent proteins, *Trends Biochem. Sci. 20*, 448−455.
2. Ormö, M., Cubitt, A. B., Kallio, K., Gross, L. A., Tsien, R. Y., and Remington, S. J. (1996) Crystal structure of the *Aequorea victoria* green fluorescent protein, *Science 273*, 1392−1395.
3. Yang, F., Moss, L. G., and Phillips, G. N. J. (1996) The molecular structure of green fluorescent protein, *Nat. Biotechnol. 14*, 1246−1251.
4. Brejc, K., Sixma, T. K., Kitts, P. A., Kain, S. R., Tsien, R. Y., Ormo, M., and Remington, S. J. (1997) Structural basis for dual excitation and photoisomerization of the *Aequorea victoria* green fluorescent protein, *Proc. Natl. Acad. Sci. U.S.A. 94*, 2306−2311.
5. Chattoraj, M., King, B. A., Bublitz, G. U., and Boxer, S. G. (1996) Ultra-fast excited state dynamics in green fluorescent protein: multiple states and proton transfer, *Proc. Natl. Acad. Sci. U.S.A. 93*, 8362−8367.
6. (a) Lossau, H., Kummer, A., Heinecke, R., Pollinger-Dammer, F., Kompa, C., Bieser, G., Jonsson, T., Silva, C. M., Yang, M. M., Youvan, D. C., and Michel-Beyerle, M. E. (1996) Proton shuttle in green fluorescent protein studied by dynamic simulations, *Chem. Phys. 213*, 1−16. (b) Kummer, A. D., Kompa, C., Lossau, H., Pollinger-Dammer, F., Michel-Beyerle, M. E., Silva, C. M., Bylina, E. J., Coleman, W. J., Yang, M. M., and Youvan, D. C. (1998) Dramatic reduction in fluorescence quantum yield in mutants of green fluorescent protein due to fast internal conversion, *Chem. Phys. 237*, 183−193.
7. Striker, G., Subramanian, V., Seidel, C. A. M., and Volkmer, A. (1999) Photochromicity and fluorescence lifetimes of green fluorescent protein, *J. Phys. Chem. B 103*, 8612−8617.
8. Winkler, K., Lindner, J. R., Subramanian, V., Jovin, T. M., and Vohringer, P. (2002) Ultrafast dynamics in the excited state of green fluorescent protein (wt) studied by frequency-resolved femtosecond pump−probe spectroscopy, *Phys. Chem. Chem. Phys. 4*, 1072−1081.
9. Litvinenko, K. L., Webber, N. M., and Meech, S. R. (2002) Ultrafast excited-state relaxation of the chromophore of the green fluorescence protein, *Bull. Chem. Soc. Jpn. 75*, 1065−1070.
10. Cotlet, M., Hofkens, J., Maus, M., Gensch, T., Van der Auweraer, M., Michiels, J., Dirix, G., Van Guyse, M., Vanderleyden, J., Visser, A. J. W. G., and De Schryver, F. C. (2001) Excited-state dynamics in the enhanced green fluorescent protein mutant probed by picosecond time-resolved single photon counting spectroscopy, *J. Phys. Chem. B 105*, 4999−5006.
11. Leiderman, P., Ben-Ziv, M., Genosar, L., Huppert, D., Solntsev, K. M., and Tolbert, L. M. (2004) Study of the long-time fluorescence tail of the green fluorescent protein, *J. Phys. Chem. B 108*, 8043−8053.
12. Weller, A. (1961) Fast reactions of excited molecules, *Prog. React. Kinet. 1*, 189−214.
13. Agmon, N. (2005) Proton pathways in green fluorescence protein, *Biophys. J. 88*, 2452−2461.
14. Leiderman, P., Huppert, D., and Agmon, N. (2006) Transition in the temperature-dependence of GFP fluorescence: from proton wires to proton exit, *Biophys. J. 90*, 1009−1018.
15. Elsliger, M. A., Wachter, R. M., Hanson, G. T., Kallio, K., and Remington, S. J. (1999) Structural and spectral response of green fluorescent protein variants to changes in pH, *Biochemistry 38*, 5296−5301.
16. Agmon, N., and Gopich, I. V. (1999) Kinetic transition in excited-state reversible reactions, *Chem. Phys. Lett. 302*, 399−404.
17. Gopich, I. V., Solntsev, K. M., and Agmon, N. (1999) Excited-state reversible geminate reaction. I. Two different lifetimes, *J. Chem. Phys. 110*, 2164−2174.
18. Zaitsev, N. K., Demyashkevich, A. B., and Kuz'min, M. G. (1980) A kinetic model of the pseudounimolecular photoprotolytical reactions in aqueous solutions, *Doklady Phys. Chem. 255*, 948−951.
19. Agmon, N., Pines, E., and Huppert, D. (1988) Geminate recombination in proton-transfer reactions. II. Comparison of diffusional and kinetic schemes, *J. Chem. Phys. 88*, 5631−5638.
20. Pines, E., Huppert, D., and Agmon, N. (1988) Geminate recombination in excited-state proton-transfer reactions: numerical solution of the Debye−Smoluchowski equation with backreaction and comparison with experimental results, *J. Chem. Phys. 88*, 5620−5630.
21. Debye, P. (1942) Reaction rates in ionic solutions, *Trans. Electrochem. Soc. 82*, 265−271.
22. Martynov, I. Yu., Demyashkevich, A. B., Uzhinov, B. M., and Kuzmin, M. G. (1977) Proton transfer reactions in excited electron states of aromatic molecules, *Russ. Chem. Rev. 46*, 1−15.
23. Rini, M., Pines, D., Magnes, B.-Z., Pines, E., and Nibbering, E. T. J. (2004) Bimodal proton transfer in acid−base reactions in water, *J. Chem. Phys. 121*, 9593−9610.
24. Leiderman, P., Genosar, L., and Huppert, D. (2005) Excited-state proton transfer: indication of three steps in the dissociation and recombination process, *J. Phys. Chem. A 109*, 5965−5977.
25. Ireland, J. F., and Wyatt, P. A. H. (1976) Acid−base properties of electronically excited states of organic molecules, *Adv. Phys. Org. Chem. 12*, 131−221.
26. Masad, A., and Huppert, D. (1991) Geminate recombination of proton transfer reactions: time-resolved fluorescence study of 1-naphthol-3,6-disulfonate, *Chem. Phys. Lett. 180*, 409−415.
27. Pines, E., Tepper, D., Magnes, B.-Z., Pines, D., and Barak, T. (1998) Competitive geminate quenching and geminate recombination reactions of 1-naphthol, *Ber. Bunsenges. Phys. Chem. 102*, 504−510.
28. Solntsev, K. M., Huppert, D., and Agmon, N. (1999) The photochemistry of "super" photoacids. Solvent effects, *J. Phys. Chem. A 103*, 6984−6997.
29. Solntsev, K. M., Huppert, D., Agmon, N., and Tolbert, L. M. (2000) Photochemistry of "super" photoacids. 2. Excited-state proton transfer in methanol/water mixtures, *J. Phys. Chem. A 104*, 4658−4669.
30. Shi, X., Abbyad, P., Shu, X., Kallio, K., Kanchanawong, P., Childs, W., Remington, A. J., and Boxer, S. G. (2007) Ultrafast excited-state dynamics in the green fluorescent protein variant S65T/H148D. 2. Unusual photophysical properties, *Biochemistry 46*, 12014−12025.
31. The broad low intensity "bump" in the response function at about 200 ps with a relative peak intensity of 0.01 is also superimposed on the experimental fluorescence signal and does not affect the analysis.
32. Shu, X., Kallio, K., Shi, X., Abbyad, P., Kanchanawong, P., Childs, W., McAnaney, T. B., Boxer, S. G., and Remington, S. J. (2007) Ultrafast excited-state dynamics in the green fluorescent protein

variant S65T/H148D. 1. Mutagenesis and structural studies, *Biochemistry 46*, 12005−12013.
33. Dong, J., Solntsev, K. M., and Tolbert, L. M. (2006) Solvatochromism of the green fluorescence protein chromophore and its derivatives, *J. Am. Chem. Soc. 128*, 12038−12039.
34. Formosinho, S. J., and Arnaut, L. G. (1993) Excited-state proton transfer reactions. II: Intramolecular reactions, *J. Photochem. Photobiol. A: Chem. 75*, 21−48.
35. Rini, M., Kummrow, A., Dreyer, J., Nibbering, E. T. J., and Elsaesser, T. (2003) Femtosecond mid-infrared spectroscopy of condensed phase hydrogen-bonded systems as a probe of structural dynamics, *Faraday Discuss. 122*, 27−40.
36. Le Gourrierec, D., Ormson, S. M., and Brown, R. G. (1994) Excited-state intramolecular proton transfer, part 2: ESIPT to oxygen, *Prog. React. Kinet. 19*, 211−275.
37. Chou, P.-T. (2001) The host/guest type of excited-state proton transfer; a general review, *J. Chin. Chem. Soc. 48*, 651−682.
38. Ameer-Beg, S., Ormson, S. M., Brown, R. G., Matousek, P., Towrie, M., Nibbering, E. T. J., Foggi, P., and Neuwahl, F. V. R. (2001) Ultrafast measurements of excited state intramolecular proton transfer (ESIPT) in room temperature solutions of 3-hydroxyflavone and derivatives, *J. Phys. Chem. A 105*, 3709−3718.
39. Lochbrunner, S., Stock, K., and Riedle, E. (2004) Direct observation of the nuclear motion during ultrafast intramolecular proton transfer, *J. Mol. Struct. 700*, 13−18.
40. Lochbrunner, S., Szeghalmi, A., Stock, K., and Schmitt, M. (2005) Ultrafast proton transfer of 1-hydroxy-2-acetonaphthone: reaction path from resonance Raman and transient absorption studies, *J. Chem. Phys. 122*, 244315.
41. Stavrov, S. S., Solntsev, K. M., Tolbert, L. M., and Huppert, D. (2006) Probing the decay coordinate of the green fluorescent protein: arrest of cis−trans isomerization by the protein significantly narrows the fluorescence spectra, *J. Am. Chem. Soc. 128*, 1540−1546.
42. Gepshtein, R., Huppert, D., and Agmon, N. (2006) Deactivation mechanism of the green fluorescent chromophore, *J. Phys. Chem. B 110*, 4434−4442.
43. Usman, A., Mohammed, O. F., Nibbering, E. T. J., Dong, J., Solntsev, K. M., and Tolbert, L. M. (2005) Excited-state structure determination of the green fluorescent protein chromophore, *J. Am. Chem. Soc. 127*, 11214−11215.
44. Solntsev, K. M., Al-Ainain, S. A., Il'ichev, Yu. V., and Kuzmin, M. G. (2005) Effects of long-chain alkyl substituents on the protolytic reactions of naphthols, *J. Photochem. Photobiol. A 175*, 178−191.
45. Pines, E., Magnes, B.-Z., and Barak, T. (2001) On-contact quenching of 1-naphtholate by geminate protons, *J. Phys. Chem. A 105*, 9674−9680.
46. Kummer, A. D., Kompa, C., Niwa, H., Hirano, T., Kojima, S., and Michel-Beyerle, M. E. (2002) Viscosity-dependent fluorescence decay of the GFP chromophore in solution due to fast internal conversion, *J. Phys. Chem. B 106*, 7554−7559.
47. Vengris, M., van Stokkum, I. H. M., He, X., Bell, A. F., Tonge, P., van Grondelle, R., and Larsen, D. S. (2004) Ultrafast excited and ground-state dynamics of the green fluorescent protein chromophore in solution, *J. Phys. Chem. A 108*, 4587−4598.
48. Vendrell, O., Gelabert, R., Moreno, M., and Lluch, J. L. (2004) Photoinduced proton transfer from the green fluorescent protein chromophore to a water molecule: analysis of the transfer coordinate, *Chem. Phys. Lett. 396*, 202−207.
49. Jung, G., Wiehler, J., and Zumbusch, A. (2005) The photophysics of green fluorescent protein: influence of the key amino acids at positions 65, 203, and 222, *Biophys. J. 88*, 1932−1947.
50. Webb, S. P., Philips, L. A., Yeh, S. W., Tolbert, L. M., and Clark, J. H. (1986) Picosecond kinetics of the excited-state, proton-transfer reaction of 1-naphthol with water, *J. Phys. Chem. 90*, 5154−5164.
51. Weber, W., Helms, V., McCammon, J. A., and Langhoff, P. W. (1999) Shedding light on the dark and weakly fluorescent states of green fluorescent proteins, *Proc. Natl. Acad. Sci. U.S.A. 96*, 6177−6182.
52. Shizuka, H. (1985) Excited-state proton-transfer reactions and proton-induced quenching of aromatic compounds, *Acc. Chem. Res. 18*, 141−147.
53. Pines, E., and Fleming, G. R. (1994) Self quenching of 1-naphthol: connection between time-resolved and steady-state measurements, *Chem. Phys. 183*, 393−402.

BI7009053